Contributions of the N- and C-Terminal Helical Segments to the Lipid-Free Structure and Lipid Interaction of Apolipoprotein A-I†

Masafumi Tanaka,‡ Padmaja Dhanasekaran,§ David Nguyen,§ Shinya Ohta,‡ Sissel Lund-Katz,§ Michael C. Phillips,*,§ and Hiroyuki Saito‡

Department of Biophysical Chemistry, Kobe Pharmaceutical University, Kobe 658-8558, Japan, and Lipid Research Group, The Children's Hospital of Philadelphia, University of Pennsylvania School of Medicine, Philadelphia, Pennsylvania 19104-4318

Received April 14, 2006; Revised Manuscript Received June 9, 2006

ABSTRACT: The tertiary structure of lipid-free apolipoprotein (apo) A-I in the monomeric state comprises two domains: a N-terminal α-helix bundle and a less organized C-terminal domain. This study examined how the N- and C-terminal segments of apoA-I (residues 1−43 and 223−243), which contain the most hydrophobic regions in the molecule and are located in opposite structural domains, contribute to the lipid-free conformation and lipid interaction. Measurements of circular dichroism in conjunction with tryptophan and 8-anilino-1-naphthalenesulfonic acid fluorescence data demonstrated that single (L230P) or triple (L230P/L233P/Y236P) proline insertions into the C-terminal α helix disrupted the organization of the C-terminal domain without affecting the stability of the N-terminal helix bundle. In contrast, proline insertion into the N terminus (Y18P) disrupted the bundle structure in the N-terminal domain, indicating that the α-helical segment in this region is part of the helix bundle. Calorimetric and gel-filtration measurements showed that disruption of the C-terminal α helix significantly reduced the enthalpy and free energy of binding of apoA-I to lipids, whereas disruption of the N-terminal α helix had only a small effect on lipid binding. Significantly, the presence of the Y18P mutation offset the negative effects of disruption/removal of the C-terminal helical domain on lipid binding, suggesting that the α helix around Y18 concealed a potential lipid-binding region in the N-terminal domain, which was exposed by the disruption of the helix-bundle structure. When these results are taken together, they indicate that the α-helical segment in the N terminus of apoA-I modulates the lipid-free structure and lipid interaction in concert with the C-terminal domain.

The anti-atherogenic function of apolipoprotein (apo)[1] A-I arises primarily from its central role in reverse cholesterol transport, the process whereby excess cholesterol is transported from cells in the periphery back to the liver (*1*−*3*). In this process, lipid-free or lipid-poor apoA-I molecules are the preferred acceptor of cholesterol and phospholipid transferred from cell membranes by the action of ATP-binding cassette transporter A1 (ABCA1) (*4*−*6*). Mutations in the ABCA1 gene lead to Tangier disease and Familial high-density lipoprotein (HDL) deficiency, characterized by a near absence of plasma HDL and premature atherosclerotic vascular disease (*7*, *8*).

Human apoA-I is a 243 amino acid protein in which exon 3 encodes an N-terminal region (residues 1−43) and the remaining region coded by exon 4 is predicted to contain eight 22-mer and two 11-mer amphipathic α helices (*9*, *10*). Studies of synthetic peptides corresponding to each of the 22-residue amphipathic segments of apoA-I have shown that the first (residues 44−65) and last (residues 220−241) repeat helices have the greatest lipid affinity (*11*). The C-terminal region of apoA-I is very hydrophobic as revealed by hydropathy analysis of the amino acid sequence (*12*) and is critical for lipid binding (*13*−*17*). Interestingly, the N-terminal region (residues 1−43) also contains a very hydrophobic segment centered around residue Y18 (*12*), suggesting that this region also has significant lipid-binding ability (*18*, *19*).

A unique conformational plasticity and flexibility in apoA-I appears to be important for its multiple functions (*20*−*24*). Recently, we have proposed that the tertiary structure of lipid-free apoA-I consists of two domains similar to apoE: an N-terminal antiparallel helix-bundle domain (residues 1−186) and a less organized C-terminal domain (187−243) (*12*, *25*). Three-dimensional models of the lipid-free apoA-I molecule based on cross-linking and mass spectrometry supported the two-domain conformation (*26*). Most recently, a crystal structure of lipid-free apoA-I at 2.4 Å resolution confirmed that the molecule is folded into two domains, comprising an N-terminal four-helix bundle formed by residues 10−187 and two C-terminal α helices (*27*).

† This work was supported by NIH Grant HL22633 and Grant-in-Aid for Scientific Research from the Japanese Ministry of Education, Culture, Sports, Science, and Technology (number 18790034).

* To whom correspondence should be addressed: The Children's Hospital of Philadelphia, Abramson Research Center, Suite 1102, 3615 Civic Center Blvd., Philadelphia, PA 19104-4318. Telephone: (215) 590-0587. Fax: (215) 590-0583. E-mail: phillipsmi@email.chop.edu.

‡ Kobe Pharmaceutical University.

§ University of Pennsylvania School of Medicine.

[1] Abbreviations: ABCA1, ATP-binding cassette transporter A1; ANS, 8-anilino-1-naphthalenesulfonic acid; apo, apolipoprotein; CD, circular dichroism; GdnHCl, guanidine hydrochloride; HDL, high-density lipoprotein; PC, phosphatidylcholine; SUV, small unilamellar vesicle; Trp, tryptophan; WT, wild type.

10.1021/bi060726t CCC: $33.50
Published on Web 08/05/2006

However, because of protein aggregation on crystallization, the α-helix content of ~80% found in the crystal structure is significantly higher than the ~50% (*14*−*16*) found for lipid-free, monomeric apoA-I in dilute solution.

Studies of apoA-I variants containing deletion or point mutations showed that the ability of apoA-I to bind lipids through the C-terminal α helix (residues 220−241) plays a key role in both phospholipid and cholesterol efflux from cells to apoA-I via ABCA1 (*28*−*32*). In contrast, ABCA1-mediated lipid efflux appears to be relatively insensitive to the organization of the N-terminal helix-bundle domain (*31*, *32*). Interestingly, apoA-I mutants lacking both the extreme N- and C-terminal regions displayed the capability of binding lipids and promoting ABCA1-mediated lipid efflux similar to full-length apoA-I (*31*, *33*), suggesting that a different structural element, which is conserved in the central helices, can substitute for the function of the C-terminal α helix in wild-type (WT) apoA-I.

To gain more insight into the molecular features controlling the two-domain structure and thereby the function of apoA-I, we examined the role of the extreme N- and C-terminal segments (residues 1−43 and 223−243) in the lipid-free organization and lipid interaction using engineered apoA-I molecules. To this end, proline residues were inserted into the N- and C-terminal regions (Y18, L230, L233, and Y236) to disrupt putative α-helical structure (*34*). Proline insertions into an α helix in a molten-globular protein are known to disrupt only the particular helix involved (*35*). The results showed that the α-helical segment centered near residue Y18 contributes to the formation of the N-terminal helix bundle in apoA-I, as suggested by the crystal structure (*27*). Interestingly, the disruption of this N-terminal α helix offset the negative effects of disruption/removal of the C-terminal helical domain on lipid binding of apoA-I, suggesting that the α helix in residues 1−43 conceals a potential lipid-binding region in the N-terminal helix-bundle domain. Our findings provide new insight into the structure−function relationships of the anti-atherogenic apoA-I molecule.

EXPERIMENTAL PROCEDURES

Materials. Ultrapure guanidine hydrochloride (GdnHCl) was obtained from MP Biomedicals (Aurora, OH). 8-Anilino-1-naphthalenesulfonic acid (ANS) was purchased from Molecular Probes (Eugene, OR). Egg phosphatidylcholine (PC) was purchased from Sigma−Aldrich (St. Louis, MO). [^{3}H]-Cholesterol and [^{14}C]-formaldehyde were purchased from Perkin−Elmer Life Sciences (Wellesley, MA). All other reagents were special-grade.

Protein Expression and Purification. Mutations in the N-terminal (Y18P), C-terminal (L230P and L230P/L233P/Y236P), or both N- and C-terminal (Y18P/L230P and Y18P/Δ190−243) domains of human apoA-I were introduced. Amino acid residues either at Y18 or L230 (/L233/Y236) were selected to be replaced by proline residues because the regions around these residues are very hydrophobic as judged from hydropathy plot analysis of the human apoA-I sequence (*12*). WT human apoA-I and engineered mutants were expressed as thioredoxin fusion proteins in the *Escherichia coli* strain BL21-DE3 and then cleaved and purified as described previously (*25*). The apoA-I preparations were at least 95% pure as assessed by sodium dodecyl sulfate−polyacrylamide gel electrophoresis (SDS−PAGE). In all experiments, apoA-I was freshly dialyzed from 6 M GdnHCl solution into the appropriate buffer before use. Protein concentrations were determined either by the Lowry procedure using bovine serum albumin (Bio-Rad) as a standard (*36*, *37*) or by absorbance measurements at 280 nm.

Preparation of Lipid Vesicles. A film of egg PC on the wall of a glass tube was dried under vacuum overnight and hydrated with 10 mM sodium phosphate buffer (pH 7.4). Small unilamellar vesicles (SUVs) were prepared by sonication and ultracentrifuged in a Beckman TLA110 rotor (51 000 rpm) for 2 h to remove larger particles and titanium debris as described (*15*). The SUV PC concentration was determined using an enzymatic assay kit for choline from Wako (Osaka, Japan). The particle diameter determined by quasi-elastic light-scattering measurements was 25 ± 5 nm in weighted average.

Circular Dichroism (CD) Spectroscopy. CD spectra were obtained using either a Jasco J-600 or an Aviv 62ADS spectropolarimeter equipped with a temperature-controlled sample holder. ApoA-I samples were dissolved at 50 μg/mL in 10 mM sodium phosphate buffer (pH 7.4). Molar ellipticity ([θ]) was calculated from the equation: $[\theta] = (\mathrm{MRW})\,\theta/10lc$, where θ is a measured ellipticity in degrees, l is the cuvette path length (0.1 or 0.2 cm), c is the protein concentration in g/mL, and the mean residue weight (MRW) is obtained from the molecular weight and the number of amino acids. The α-helix contents were calculated from the equation using [θ] at 222 nm: percent α helix $= [(-[\theta]_{222} + 3000)/(36\,000 + 3000)] \times 100$ (*38*). For thermal denaturation experiments, the changes in $[\theta]_{222}$ were monitored as the sample was heated at 1 °C/min over the temperature range of 20−85 °C. For chemical denaturation experiments, samples were preincubated with given concentrations of GdnHCl overnight at 4 °C. Denaturation parameters were calculated as described (*39*). For lipid binding experiments, apoA-I was incubated with SUVs (PC/apoA-I weight ratio of 60:1) for 1 h prior to the measurement (*15*).

Fluorescence Measurements. All fluorescence measurements were carried out at 25 °C using a Hitachi F-4500 spectrophotometer. For chemical denaturation experiments, the emission spectra of tryptophan (Trp) were recorded from 300 to 420 nm at the excitation wavelength of 295 nm. Proteins at a concentration of 50 μg/mL were preincubated with GdnHCl as described above. The extent of ANS binding to hydrophobic sites on a protein was determined by measuring ANS fluorescence spectra recorded from 400 to 600 nm at the excitation wavelength of 395 nm in the absence or presence of 50 μg/mL protein and an excess of ANS (250 μM) (*25*, *39*).

Binding of ApoA-I to SUVs. The binding of apoA-I to SUVs was assayed by gel-filtration chromatography as described (*15*). SUVs and apoA-I were labeled with trace amounts of [^{3}H]-cholesterol and [^{14}C]-formaldehyde, respectively. After incubation of various concentrations of apoA-I (10−100 μg/mL) with SUVs (1 mg/mL egg PC), the mixtures were applied to a Sepharose CL-6B column and 0.5 mL fractions were collected. Under our experimental conditions, bound apoA-I did not disrupt the structural integrity of the vesicles (*15*). Aliquots of each fraction were counted using liquid scintillation procedures to determine

Table 1: α-Helix Content and Thermal Denaturation Parameters of ApoA-I Proline Mutants

		thermal denaturation		
	α helix[a] (%)	T_m[b] (°C)	cooperativity index	ΔH_v[c] (kcal/mol)
WT[d]	44 ± 4	60	7.8	33
Y18P	44 ± 4	60	7.5	32
L230P	39 ± 2	56	9.8	41
L230P/L233P/Y236P	46 ± 5	57	10.6	43
Y18P/L230P	42 ± 5	52	6.8	33
Y18P/Δ190−243	43 ± 4	49	5.5	30

[a] Mean ± SD from at least three independent experiments. [b] The reproducibility in T_m is ±1.0 °C. [c] Estimated error is within ±0.5 kcal/mol. [d] Data are added from ref *25*.

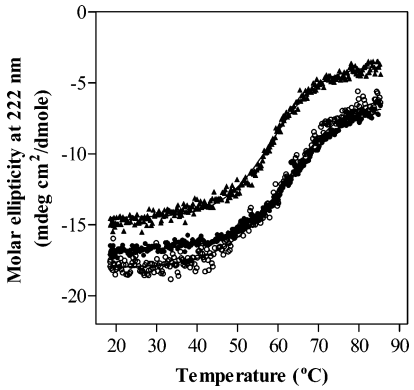

FIGURE 1: Thermal denaturation curves of WT (●), Y18P (○), and L230P (▲) apoA-I monitored by the molar ellipticity at 222 nm. Protein concentrations were 50 μg/mL.

the levels of labeled SUVs and apoA-I. Binding isotherms were obtained by nonlinear regression analysis (GraphPad Prism) using a one-site-binding model. The dissociation constant, K_d, was determined as the fitting parameter.

Isothermal Titration Calorimetry (ITC). Enthalpies of apoA-I binding to SUVs were measured using a MicroCal MCS isothermal titration calorimeter at 25 °C as described (*15*). Measurements were carried out by titrating 8 μL aliquots of apoA-I sample (0.8 mg/mL) into the cell (1.35 mL) containing an excess of SUVs (15 mM) to ensure the complete binding of apoA-I to SUVs. Samples were degassed under vacuum prior to use. Mixing of reactants was accomplished by rotating the syringe paddle at 400 rpm. Enthalpies of apoA-I binding to SUVs were corrected for heats of apoA-I dilution and dissociation at 25 °C; these values were determined by titrating apoA-I into buffer alone.

RESULTS

Secondary Structure and Thermal Unfolding of ApoA-I Variants. The lipid-free structures of apoA-I variants were analyzed by far-UV CD spectroscopy. All apoA-I variants exhibited typical CD spectra for an α-helical structure (data not shown), and α-helix contents were calculated from the molar ellipticity at 222 nm. All of the apoA-I proline mutants showed similar α-helix contents compared to WT apoA-I (Table 1), suggesting that proline substitution acted only to partially break or bend the α helix so that the α-helix content of the entire protein was not affected much (*40*).

Figure 1 shows the thermal denaturation curves of WT, Y18P, and L230P apoA-I monitored by the change in molar ellipticity at 222 nm over the temperature range of 20−85 °C. In comparison to the WT, almost no differences were observed in the denaturation curve of Y18P, whereas the L230P mutation increased the cooperativity of unfolding as revealed by the shape of the curve (Figure 1). The midpoint temperature, T_m, the cooperativity index, and the van't Hoff enthalpy, ΔH_v, of thermal unfolding are summarized in Table 1. Mutations in both the N- and C-terminal domains caused a significant decrease in T_m and cooperativity index compared to the WT, implying destabilization of the protein structure. Because the C-terminal mutants increased the cooperativity and enthalpy of unfolding, the destabilizing effect in the double mutants is likely to come mainly from the N-terminal part, although the Y18P mutation itself had little effect on the thermodynamic parameters.

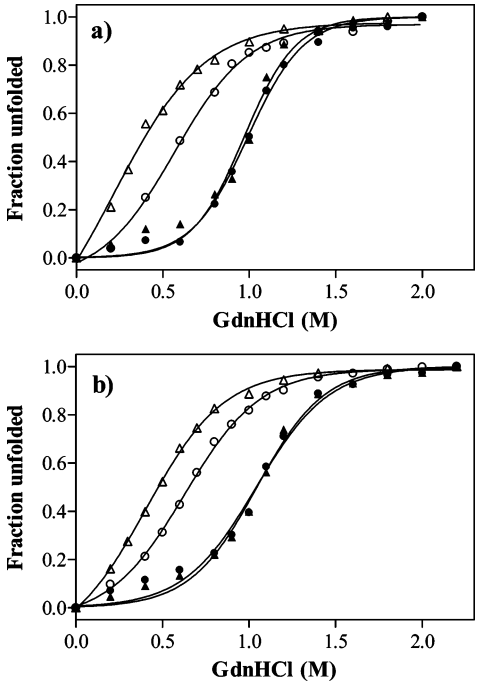

FIGURE 2: GdnHCl-induced denaturation curves of WT (●), Y18P (○), L230P (▲), and Y18P/L230P (△) apoA-I monitored by (a) the molar ellipticity or (b) Trp fluorescence intensity. Protein concentrations were 50 μg/mL. The denaturation curves are representative of at least two separate experiments.

GdnHCl Denaturation of ApoA-I Variants. GdnHCl-induced denaturation profiles were monitored either by CD or Trp fluorescence measurements. The changes in molar ellipticity at 222 nm or Trp fluorescence intensity at 335 nm were used to monitor the denaturation that occurred as a two-state process (*38*). Because the four Trp residues in the apoA-I molecule are located in the N-terminal half (positions 8, 50, 72, and 108) of the protein, the change in Trp fluorescence only reflects the unfolding of the N-terminal domain (*25*). In contrast, the change in molar ellipticity at 222 nm reflects the unfolding of the entire protein based on the secondary structure. Parts a and b of Figure 2 show the denaturation curves of WT, Y18P, L230P, and Y18P/L230P apoA-I determined by CD or Trp fluorescence measurements, respectively. In both measurements, the L230P mutation did not alter the denaturation profiles, whereas the Y18P variant showed a marked shift toward lower GdnHCl concentrations compared to the WT (parts a and b of Figure 2). The similar denaturation profiles obtained from CD and Trp fluorescence indicate that disruption of the secondary and tertiary structure

Table 2: Parameters of GdnHCl-Induced Denaturation and ANS Binding of ApoA-I Proline Mutants

	molar ellipticity			fluorescence intensity			
	$\Delta G_D°$ (kcal/mol)	m	$D_{1/2}$ (M)	$\Delta G_D°$ (kcal/mol)	m	$D_{1/2}$ (M)	ANS fluorescence[a]
WT	3.4 ± 0.2	3.4	1.01 ± 0.11	3.1 ± 0.2	3.0	1.05 ± 0.13	1.0
Y18P	1.1 ± 0.2	1.9	0.58 ± 0.15	1.6 ± 0.1	2.4	0.67 ± 0.05	1.7
L230P	3.6 ± 0.3	3.8	0.95 ± 0.13	2.9 ± 0.2	2.8	1.04 ± 0.11	0.6
L230P/L233P/Y236P	4.0 ± 0.6	3.8	1.06 ± 0.30	2.9 ± 0.1	2.7	1.09 ± 0.10	0.5
Y18P/L230P	0.8 ± 0.1	2.0	0.41 ± 0.11	1.1 ± 0.1	2.3	0.49 ± 0.07	1.5
Y18P/Δ190−243	1.1 ± 0.1	2.4	0.48 ± 0.08	1.6 ± 0.2	2.5	0.64 ± 0.12	1.5

[a] Values are relative to the WT. Estimated error is within ±0.1.

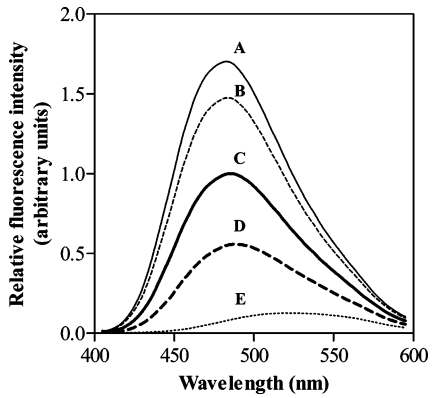

FIGURE 3: ANS fluorescence spectra of ANS bound to apoA-I variants. Fluorescence intensities are normalized to the maximum fluorescence observed with WT apoA-I. (A) Y18P, (B) Y18P/L230P, (C) WT, (D) L230P, and (E) free ANS. Protein and ANS concentrations were 50 μg/mL and 250 μM, respectively.

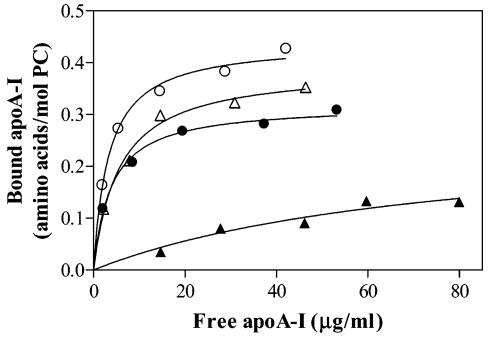

FIGURE 4: Binding isotherms of WT (●), Y18P (○), Δ190−243 (▲), and Y18P/Δ190−243 (△) apoA-I to egg PC SUVs. The binding isotherms are representative of at least two separate experiments. The binding curves were obtained by nonlinear regression fitting to a one-binding-site model.

occurs simultaneously. The conformational stability, $\Delta G_D°$, the midpoint of chemical denaturation, $D_{1/2}$, and m values determined from the linear plots of the Gibbs free energy, ΔG_D, against the GdnHCl concentration, are listed in Table 2. The L230P and L230P/L233P/Y236P variants yielded similar values of denaturation parameters to WT apoA-I. In contrast, all Y18 mutants (Y18P, Y18P/L230P, and Y18P/Δ190−243) exhibited significantly decreased $\Delta G_D°$, $D_{1/2}$, and m values, indicating a reduction in the stability of the N-terminal bundle structure, consistent with the crystal structure in which the α helix around Y18 is involved in the formation of the N-terminal helix-bundle structure (*27*).

ANS Binding. An ANS-binding study was performed to compare the exposure of hydrophobic regions in the apoA-I variants to the aqueous environment. In comparison to ANS fluorescence in the absence of a protein, WT apoA-I induced about a 10-fold increase in the fluorescence quantum yield (Figure 3), suggesting the presence of an ANS-accessible hydrophobic surface in apoA-I (*25*, *33*, *41*). As shown in Table 2, the Y18P mutation and double mutations (Y18P/L230P and Y18P/Δ190−243) led to large enhancements in ANS fluorescence compared to the WT, indicating that the incorporation of a proline residue at position 18 exposes more hydrophobic surface by the disruption of the helix-bundle structure. On the other hand, the L230P and L230P/L233P/Y236P mutations decreased the ANS fluorescence in a manner similar to the mutations Δ223−243 and Δ190−243 (*25*), suggesting that disruption of the α helix in the C-terminal domain decreases the exposed hydrophobic surface available for ANS binding relative to WT apoA-I. Likewise, the double mutations (Y18P/L230P and Y18P/Δ190−243) decreased the ANS fluorescence compared to that of the Y18P variant, although the extent of reduction in ANS fluorescence was much smaller than those caused by the same C-terminal mutations in the WT molecule.

Interactions of ApoA-I Variants with Lipid. Figure 4 shows the binding isotherms of WT, Y18P, Δ190−243, and Y18P/Δ190−243 apoA-I to egg PC SUVs obtained by a gel-filtration method. The dissociation constants, K_d, which reflect the binding affinities, are listed in Table 3. The Y18P variant bound to SUVs with a somewhat higher affinity than WT. In contrast, the L230P mutation slightly decreased the binding affinity. The binding isotherm of the L230P/L233P/Y236P mutant, like that of the Δ223−243 mutant in the previous study (*15*), did not clearly saturate in the concentration range studied (data not shown), but the binding affinity of the triple proline mutant to SUVs was considerably reduced compared to WT apoA-I. This observation indicates that disruption of the α-helix structure in the C-terminal region impairs lipid binding (*42*). Surprisingly, the Y18P/Δ190−243 mutant, which entirely lacks the C-terminal domain, showed high-affinity binding comparable to the WT, suggesting that regions other than the C terminus in apoA-I can facilitate interaction with lipid. In contrast, K_d for the Y18P/L230P mutant was similar to that for the L230P mutant.

To further examine the effects of the mutations on the interaction of apoA-I with lipids, far-UV CD measurements were performed in the absence or presence of egg PC SUVs. The increase in the number of α-helical residues upon binding to SUVs is thought to be the driving force for high-affinity binding of apoA-I to lipids (*15*, *43*). Figure 5a shows far-UV CD spectra of the Y18P/L230P variant in the lipid-free state and bound to SUVs. Figure 5b summarizes the increases in the number of α-helical residues for all apoA-I variants. Binding to lipid increased the α-helical residues

Table 3: Thermodynamic Parameters of ApoA-I Binding to SUVs

	K_d (μg/mL)	ΔH (kcal/mol)	ΔG (kcal/mol)	ΔS (cal mol^{-1} K^{-1})
WT[a]	4.6 ± 1.8	−92.6 ± 5.3	−11.6 ± 0.2	−272 ± 18
Y18P	2.1 ± 1.0	−93.9 ± 5.3	−12.1 ± 0.3	−275 ± 19
L230P	10.1 ± 4.3	−69.7 ± 3.7	−11.2 ± 0.3	−196 ± 13
L230P/L233P/Y236P	19.8 ± 20.9	−56.1 ± 4.8	−10.0 ± 0.2	−155 ± 17
Y18P/L230P	9.9 ± 3.9	−138.5 ± 10.4	−11.2 ± 0.2	−418 ± 36
Δ190−243[a]	68.7 ± 36.8	−39.2 ± 2.8	−9.9 ± 0.5	−98 ± 11
Y18P/Δ190−243	2.0 ± 1.4	−111.4 ± 5.4	−12.0 ± 0.5	−334 ± 20

[a] Data are added from ref *15*.

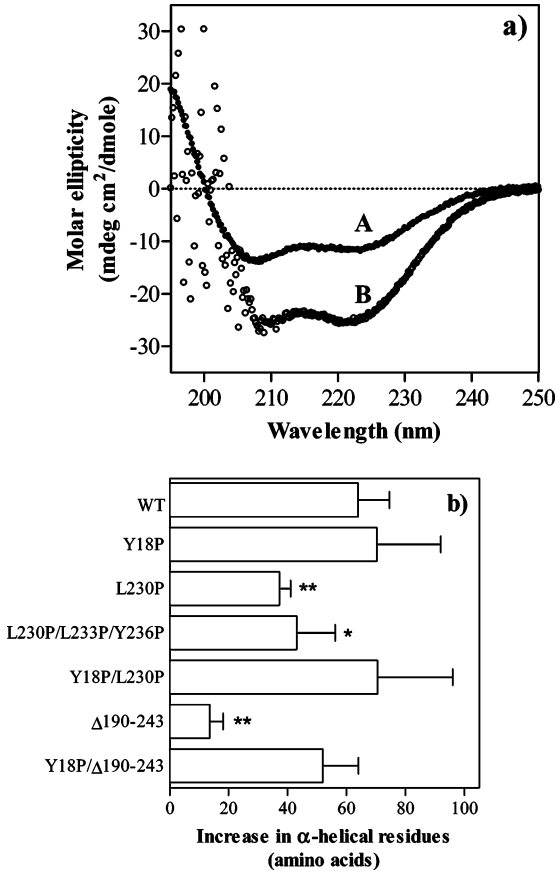

FIGURE 5: (a) Far-UV CD spectra of Y18P/L230P apoA-I in the absence (A) and presence (B) of egg PC SUVs. The protein concentration was 50 μg/mL. In the mixture of apoA-I and SUVs, the PC/protein weight ratio was set to 60:1. Mixtures were incubated for 1 h prior to the measurement. (b) Comparison of the increases in α-helical residues in the apoA-I variants upon binding to SUVs [mean ± standard deviation (SD)]. Unpaired *t* tests were performed to determine the significant differences from WT apoA-I. (* and **) Significantly different at $p < 0.05$ and 0.01, respectively.

similarly in the Y18P variant and WT apoA-I, whereas the increases in α-helical residues for the L230P and L230P/L233P/Y236P variants were significantly smaller than that for WT. The Y18P/L230P and Y18P/Δ190−243 variants increased their α-helical residues similar to WT apoA-I upon lipid binding.

ITC measurements were carried out to obtain the thermodynamic parameters characterizing the binding of apoA-I to egg PC SUVs because the enthalpy change associated with α-helix formation favors apoA-I binding to SUVs (*15*, *43*). The entropy of binding (ΔS) was calculated from the binding enthalpy (ΔH) obtained directly from ITC measurements and the free energy (ΔG) calculated using the binding constant ($1/K_d$). Table 3 summarizes the thermodynamic parameters for the binding of the apoA-I variants to egg PC SUVs. The Y18P variant generated an exothermic heat similar to the WT but unlike Δ1−43 apoA-I, which exhibited a large decrease in the binding enthalpy (*15*). This implies that some amino acids in the region encompassing residues 1−43, other than residues immediately around Y18, form α-helix structure upon lipid binding. The L230P and L230P/L233P/Y236P mutations decreased the binding enthalpy as predicted from the CD results (Figure 5b), confirming the important role in lipid binding of α-helix structure formation in the C-terminal region. Significantly, binding of the double mutants (Y18P/L230P and Y18P/Δ190−243) to SUVs was accompanied by a large exothermic heat despite the disruption/deletion in the C-terminal domain, suggesting that destabilizing the N-terminal helix-bundle structure by proline insertion at Y18 diminishes the negative effects of the C-terminal modifications on lipid binding.

DISCUSSION

The crystal structure of full-length apoA-I reported recently at 2.4 Å resolution provides a structural template for understanding the structure of lipid-free apoA-I (*27*), although crystallization resulted in a helical content closer to that found in the lipid-bound state. At this stage, it is not known which residues of apoA-I are involved in α-helix formation in the monomeric, lipid-free state. We previously described the two-domain structure of human apoA-I using a series of deletion mutants (*25*). The proline insertions in the present study provided complementary structural information to that obtained with corresponding deletion mutants. Here, using proline point mutations, we discuss the roles of the N- and C-terminal helical regions of apoA-I in the lipid-free structure and lipid interaction.

Roles of the N- and C-Terminal Domains in the Lipid-Free Conformation of ApoA-I. The first 43 residues of human apoA-I are encoded by exon 3, and the sequence of this region is highly conserved among mammals (*44*). In contrast to residues 44−243, which contain tandem 11 or 22 amino acid residue repeats, residues 1−43 contain undefined structure and, in fact, a synthetic peptide study showed that the peptide corresponding to residues 1−44 is unfolded in aqueous solution (*19*). However, our previous results with the Δ1−43 mutation indicated that this region in the apoA-I molecule contains about 50% helical structure (*25*). GdnHCl-induced denaturation studies indicate that insertion of a proline residue at position Y18 disrupts the N-terminal helix-bundle structure (Figure 2), which is corroborated by the increase in ANS fluorescence of the Y18P variants (Figure 3). The perturbation of the helix-bundle structure by the Y18P mutation presumably occurs because the residues around Y18 form an α-helix structure that helps to stabilize

the N-terminal domain by incorporation into the helix bundle. This concept is consistent with the crystal structure in which the α-helical segment spanning residues 1−43 forms an integral part of the N-terminal helix bundle (*27*).

A comparison of thermal and GdnHCl-induced denaturation revealed that different unfolding processes proceed during denaturation. Unlike the destabilization seen with GdnHCl-induced denaturation, the Y18P mutation had a negligible effect on the stability of the helical structure in thermal denaturation experiments (Table 1), consistent with previous observations for N-terminal deletion mutants (*25*, *31*). Because the N-terminal Y18P mutation combined with C-terminal modifications dramatically decreased the stability of α helices in the protein (Table 1), it appears that the C-terminal domain somehow influences the stability of the N-terminal helix bundle through interactions between the N- and C-terminal segments (*26*, *45*−*47*). Indeed, essentially all two-state folding proteins have their N- and C-terminal segments in contact, playing specific roles in protein folding and stability (*48*).

Proline insertions into the C-terminal domain led to a reduction in ANS fluorescence. The degree of reduction in the fluorescence by the proline insertions was as much as that caused by the C-terminal deletion mutations (*25*), suggesting that the disruption of the C-terminal helix eliminates the hydrophobic surface available for ANS binding. It is noteworthy that the decreases in ANS fluorescence for the double mutants (Y18P/Δ190−243 and Y18P/L230P) relative to Y18P were smaller than that for the C-terminal disruption/truncation mutants (L230P and Δ190−243) relative to the WT (Table 2). These results are reasonably explained by the idea that the Y18P mutation has two distinct influences on the apoA-I structure. The major effect is to disrupt the N-terminal helix-bundle structure, as discussed above. Another effect is to modify an N- and C-terminal domain interaction (*45*, *49*) so that the amount of exposed hydrophobic surface arising from the domain interaction is decreased. In addition, a comparison of the thermal or GdnHCl-induced denaturation data for the Y18P and Y18P/L230P mutants (Tables 1 and 2) indicates that disruption of both terminal regions by proline insertion leads to destabilization of the double-mutant apoA-I molecule. Thus, the N-terminal region of apoA-I is part of the N-terminal helical-bundle structure and is involved in the interaction with the C-terminal domain that stabilizes the molecule.

Exposure of the hydrophobic surfaces of amphipathic α helices by destabilizing the apoA-I N-terminal helix bundle in plasma would be unfavorable because it could lead to protein aggregation and fibril formation through hydrophobic interaction among α helices (*50*). Several naturally occurring mutations in the N-terminal domain of apoA-I have been identified to be associated with amyloidosis (*44*, *51*). The amyloid deposits composed of N-terminal fragments (∼90 residues) of the mutant apoA-I are found in some individuals with amyloidosis (*52*). It has been proposed that lipid-free apoC-II forms partially folded intermediates prone to amyloid formation (*53*, *54*). It is possible that the mutations in the N-terminal domain of apoA-I lead to the unfolding of the bundle structure, which gives rise to a higher susceptibility to protease digestion causing the formation of amyloid deposits. Further studies are needed to connect the stability of the N-terminal helix-bundle domain of apoA-I with the formation of amyloid deposits.

Roles of the N- and C-Terminal Domains in the ApoA-I Binding to Lipid. According to the two-step mechanism for apoA-I binding to lipid particles, apoA-I initially binds to lipid through the C-terminal domain, followed by a conformational opening of the helix bundle in the N-terminal domain (*12*). The C-terminal helix is critical as reflected by the effects of either its deletion (*25*) or disruption by proline insertion (Table 3). The interaction of the C-terminal domain with lipid is accompanied by an increase in α-helical structure, in which the random-coil region between residues 190−220 forms α-helix structure upon lipid binding (*15*, *55*). The tendency to a larger increase in the number of α-helical residues in Y18P/L230P compared to Y18P/Δ190−243 (Figure 5b) supports this idea. The central region (residues 123−142), which predominantly contains a significant amount of nonhelical structure (*56*, *57*), also appears to become α-helical upon the opening of the N-terminal helix bundle after lipid binding (*15*). In addition, the observation that the apoA-I (1−44) peptide can form discoidal structures in which 60% of the random-coil region folds into α helix (*19*) suggests that residues 1−43 have a role in lipid binding (*15*, *16*). This idea is supported by the data in Figure 5b, comparing the increases in numbers of α-helical residues that are induced upon lipid binding. Thus, the results for the Δ190−243 apoA-I variant suggest that about 15 residues become helical in the N-terminal helix-bundle domain. In the double mutant Y18P/Δ190−243, which has a relatively destabilized N-terminal helix bundle (Tables 1 and 2), the equivalent number is 55 residues. The question then arises as to what proportion of the difference of approximately 40 residues is contributed by the region spanning amino acids 1−43? This proportion seems to be about half because only some 20 residues in the 1−43 region are available to become α-helical upon lipid interaction because, as noted above, about 50% are already α-helical in the monomeric, lipid-free apoA-I molecule (*25*).

The results of apoA-I binding to egg PC SUVs in Figure 4 indicate that mutations in both the N- and C-terminal domains restore the lipid-binding capability despite the disruption/removal in the C-terminal domain, which is critical for lipid binding (*13*−*17*). This observation is consistent with a recent finding showing that combined N- and C-terminal truncated apoA-I, apoA-I (44−186), possesses lipid-binding capability comparable to WT apoA-I (*33*). Such double-deletion mutations in apoA-I also restore the ABCA1-mediated lipid efflux activity that was lost with only the C-terminal deletion (*31*). One possible region that is capable of substituting for the lipid-binding function of the C-terminal domain in full-length apoA-I is that spanning residues 44−65, because the α-helix spanning these residues has a strong lipid affinity comparable to the C-terminal helix (*11*). Thus, it is plausible that a conformational rearrangement in residues around Y18 exposes the latent lipid-binding domain in residues 44−65, which is concealed in the α-helix-bundle structure, to promote lipid binding and ABCA1-mediated lipid efflux. In contrast to the C-terminal α helix (residues 220−241), the role of the α helix spanning residues 44−65 in the function of apoA-I is not well-understood. Although deletion of residues 44−65 has a minor effect on ABCA1-mediated lipid efflux (*31*, *32*), the helix translocation mutant

study showed that residues 44−65 can substitute for the lipid-efflux ability of residues 220−241 (*29*). In the lipid-binding/solubilization step of ABCA1-mediated efflux of cellular lipids to apoA-I, the N-terminal α helices including residues 44−65 are thought to play a role in helix penetration and microsolubilization process (*28*, *32*) probably through the opening of the N-terminal helix bundle (*23*).

It is proposed that apoA-IV, which belongs to the same gene family as apoA-I, forms a single structural domain similar to the N-terminal helical bundle of apoA-I (*58*). Although apoA-IV binds to lipid with a relatively low affinity, mutations in the C-terminal region loosen the packing of the helical bundle and enhance the lipid-binding capability (*59*). Thus, the C-terminal region of apoA-IV constrains its ability to associate with lipid by stabilizing the folded helical-bundle structure (*59*). It is conceivable that residues 1−43 hamper the lipid binding of residues 44−65 in the N-terminal helical bundle of apoA-I in a similar manner.

In summary, the current study has explained prior work (*41*) showing that removal of residues 1−43 destabilizes the apoA-I molecule by demonstrating that the α-helical structure in residues 1−43 contributes to the stabilization of the N-terminal helix-bundle structure. Heretofore, the structure adopted in the apoA-I molecule by residues 1−43 that are coded for by exon 3 has been ambiguous. Disruption of the helix-bundle structure by mutations in the N-terminal region appears to expose a latent N-terminal lipid-binding region, which may facilitate the formation of amyloid fibrils.

ACKNOWLEDGMENT

The authors thank Drs. Saburo Aimoto and Toru Kawakami (Institute for Protein Research, Osaka University, Japan) for their help with ITC measurements.

REFERENCES

1. Fielding, C. J., and Fielding, P. E. (2001) Cellular cholesterol efflux, *Biochim. Biophys. Acta 1533*, 175−189.
2. Yancey, P. G., Bortnick, A. E., Kellner-Weibel, G., de la Llera-Moya, M., Phillips, M. C., and Rothblat, G. H. (2003) Importance of different pathways of cellular cholesterol efflux, *Arterioscler., Thromb., Vasc. Biol. 23*, 712−719.
3. Lewis, G. F., and Rader, D. J. (2005) New insights into the regulation of HDL metabolism and reverse cholesterol transport, *Circ. Res. 96*, 1221−1232.
4. Oram, J. F. (2003) HDL apolipoproteins and ABCA1: Partners in the removal of excess cellular cholesterol, *Arterioscler., Thromb., Vasc. Biol. 23*, 720−727.
5. Lee, J. Y., and Parks, J. S. (2005) ATP-binding cassette transporter AI and its role in HDL formation, *Curr. Opin. Lipidol. 16*, 19−25.
6. Yokoyama, S. (2006) Assembly of high-density lipoprotein, *Arterioscler., Thromb., Vasc. Biol. 26*, 20−27.
7. Oram, J. F. (2000) Tangier disease and ABCA1, *Biochim. Biophys. Acta 1529*, 321−330.
8. Singaraja, R. R., Brunham, L. R., Visscher, H., Kastelein, J. J., and Hayden, M. R. (2003) Efflux and atherosclerosis: The clinical and biochemical impact of variations in the ABCA1 gene, *Arterioscler., Thromb., Vasc. Biol. 23*, 1322−1332.
9. Li, W. H., Tanimura, M., Luo, C. C., Datta, S., and Chan, L. (1988) The apolipoprotein multigene family: Biosynthesis, structure, structure−function relationships, and evolution, *J. Lipid Res. 29*, 245−271.
10. Segrest, J. P., Jones, M. K., De Loof, H., Brouillette, C. G., Venkatachalapathi, Y. V., and Anantharamaiah, G. M. (1992) The amphipathic helix in the exchangeable apolipoproteins: A review of secondary structure and function, *J. Lipid Res. 33*, 141−166
11. Palgunachari, M. N., Mishra, V. K., Lund-Katz, S., Phillips, M. C., Adeyeye, S. O., Alluri, S., Anantharamaiah, G. M., and Segrest, J. P. (1996) Only the two end helixes of eight tandem amphipathic helical domains of human apo A-I have significant lipid affinity. Implications for HDL assembly, *Arterioscler., Thromb., Vasc. Biol. 16*, 328−338.
12. Saito, H., Lund-Katz, S., and Phillips, M. C. (2004) Contributions of domain structure and lipid interaction to the functionality of exchangeable human apolipoproteins, *Prog. Lipid Res. 43*, 350−380.
13. Holvoet, P., Zhao, Z., Vanloo, B., Vos, R., Deridder, E., Dhoest, A., Taveirne, J., Brouwers, E., Demarsin, E., Engelborghs, Y., Rosseneu, M., Collen, D., and Brasseur, R. (1995) Phospholipid binding and lecithin-cholesterol acyltransferase activation properties of apolipoprotein A-I mutants, *Biochemistry 34*, 13334−13342.
14. Davidson, W. S., Hazlett, T., Mantulin, W. W., and Jonas, A. (1996) The role of apolipoprotein AI domains in lipid binding, *Proc. Natl. Acad. Sci. U.S.A. 93*, 13605−13610.
15. Saito, H., Dhanasekaran, P., Nguyen, D., Deridder, E., Holvoet, P., Lund-Katz, S., and Phillips, M. C. (2004) α-Helix formation is required for high affinity binding of human apolipoprotein A-I to lipids, *J. Biol. Chem. 279*, 20974−20981.
16. Fang, Y., Gursky, O., and Atkinson, D. (2003) Lipid-binding studies of human apolipoprotein A-I and its terminally truncated mutants, *Biochemistry 42*, 13260−13268.
17. Laccotripe, M., Makrides, S. C., Jonas, A., Zannis, V. I. (1997) The carboxyl-terminal hydrophobic residues of apolipoprotein A-I affect its rate of phospholipid binding and its association with high-density lipoprotein, *J. Biol. Chem. 272*, 17511−17522.
18. Mishra, V. K., Palgunachari, M. N., Datta, G., Phillips, M. C., Lund-Katz, S., Adeyeye, S. O., Segrest, J. P., and Anantharamaiah, G. M. (1998) Studies of synthetic peptides of human apolipoprotein A-I containing tandem amphipathic α-helixes, *Biochemistry 37*, 10313−10324.
19. Zhu, H. L., and Atkinson, D. (2004) Conformation and lipid binding of the N-terminal (1−44) domain of human apolipoprotein A-I, *Biochemistry 43*, 13156−13164.
20. Narayanaswami, V., and Ryan, R. O. (2000) Molecular basis of exchangeable apolipoprotein function, *Biochim. Biophys. Acta 1483*, 15−36.
21. Brouillette, C. G., Anantharamaiah, G. M., Engler, J. A., and Borhani, D. W. (2001) Structural models of human apolipoprotein A-I: A critical analysis and review, *Biochim. Biophys. Acta 1531*, 4−46.
22. Lund-Katz, S., Liu, L., Thuahnai, S. T., and Phillips, M. C. (2003) High-density lipoprotein structure, *Front. Biosci. 8*, d1044−d1054.
23. Marcel, Y. L., and Kiss, R. S. (2003) Structure−function relationships of apolipoprotein A-I: A flexible protein with dynamic lipid associations, *Curr. Opin. Lipidol. 14*, 151−157.
24. Gursky, O. (2005) Apolipoprotein structure and dynamics, *Curr. Opin. Lipidol. 16*, 287−294.
25. Saito, H., Dhanasekaran, P., Nguyen, D., Holvoet, P., Lund-Katz, S., and Phillips, M. C. (2003) Domain structure and lipid interaction in human apolipoproteins A-I and E, a general model, *J. Biol. Chem. 278*, 23227−23232.
26. Silva, R. A., Hilliard, G. M., Fang, J., Macha, S., and Davidson, W. S. (2005) A three-dimensional molecular model of lipid-free apolipoprotein A-I determined by cross-linking/mass spectrometry and sequence threading, *Biochemistry 44*, 2759−2769.
27. Ajees, A. A., Anantharamaiah, G. M., Mishra, V. K., Hussain, M. M., and Murthy, H. M. (2006) Crystal structure of human apolipoprotein A-I: Insights into its protective effect against cardiovascular diseases, *Proc. Natl. Acad. Sci. U.S.A. 103*, 2126−2131.
28. Gillotte, K. L., Zaiou, M., Lund-Katz, S., Anantharamaiah, G. M., Holvoet, P., Dhoest, A., Palgunachari, M. N., Segrest, J. P., Weisgraber, K. H., Rothblat, G. H., and Phillips, M. C. (1999) Apolipoprotein-mediated plasma membrane microsolubilization. Role of lipid affinity and membrane penetration in the efflux of cellular cholesterol and phospholipids, *J. Biol. Chem. 274*, 2021−2028.
29. Panagotopulos, S. E., Witting, S. R., Horace, E. M., Hui, D. Y., Maiorano, J. N., and Davidson, W. S. (2002) The role of apolipoprotein A-I helix 10 in apolipoprotein-mediated cholesterol efflux via the ATP-binding cassette transporter ABCA1, *J. Biol. Chem. 277*, 39477−39484.
30. Favari, E., Bernini, F., Tarugi, P., Franceschini, G., and Calabresi, L. (2002) The C-terminal domain of apolipoprotein A-I is involved

in ABCA1-driven phospholipid and cholesterol efflux, *Biochem. Biophys. Res. Commun. 299*, 801−805.
31. Chroni, A., Liu, T., Gorshkova, I., Kan, H. Y., Uehara, Y., von Eckardstein, A., and Zannis, V. I. (2003) The central helices of ApoA-I can promote ATP-binding cassette transporter A1 (ABCA1)-mediated lipid efflux. Amino acid residues 220−231 of the wild-type ApoA-I are required for lipid efflux in vitro and high-density lipoprotein formation in vivo, *J. Biol. Chem. 278*, 6719−6730.
32. Vedhachalam, C., Liu, L., Nickel, M., Dhanasekaran, P., Anantharamaiah, G. M., Lund-Katz, S., Rothblat, G. H., and Phillips, M. C. (2004) Influence of ApoA-I structure on the ABCA1-mediated efflux of cellular lipids, *J. Biol. Chem. 279*, 49931−49939.
33. Beckstead, J. A., Block, B. L., Bielicki, J. K., Kay, C. M., Oda, M. N., and Ryan, R. O. (2005) Combined N- and C-terminal truncation of human apolipoprotein A-I yields a folded, functional central domain, *Biochemistry 44*, 4591−4599.
34. Chou, P. Y., and Fasman, G. D. (1974) Prediction of protein conformation, *Biochemistry 13*, 222−245.
35. Schulman, B. A., and Kim, P. S. (1996) Proline scanning mutagenesis of a molten globule reveals non-cooperative formation of a protein's overall topology, *Nat. Struct. Biol. 3*, 682−687.
36. Lowry, O. H., Rosebrough, N. J., Farr, A. L., and Randall, R. J. (1951) Protein measurement with the Folin phenol reagent, *J. Biol. Chem. 193*, 265−275.
37. Markwell, M. A., Haas, S. M., Bieber, L. L., and Tolbert, N. E. (1978) A modification of the Lowry procedure to simplify protein determination in membrane and lipoprotein samples, *Anal. Biochem. 87*, 206−210.
38. Morrow, J. A., Segall, M. L., Lund-Katz, S., Phillips, M. C., Knapp, M., Rupp, B., and Weisgraber, K. H. (2000) Differences in stability among the human apolipoprotein E isoforms determined by the amino-terminal domain, *Biochemistry 39*, 11657−11666.
39. Tanaka, M., Vedhachalam, C., Sakamoto, T., Dhanasekaran, P., Phillips, M. C., Lund-Katz, S., and Saito H. (2006) Effect of carboxyl-terminal truncation on structure and lipid interaction of human apolipoprotein E4, *Biochemistry 45*, 4240−4247.
40. Li, S.-C., Goto, N. K., Williams, K. A., and Deber, C. M. (1996) α-Helical, but not β-sheet, propensity of proline is determined by peptide environment, *Proc. Natl. Acad. Sci. U.S.A. 93*, 6676−6681.
41. Rogers, D. P., Brouillette, C. G., Engler, J. A., Tendian, S. W., Roberts, L., Mishra, V. K., Anantharamaiah, G. M., Lund-Katz, S., Phillips, M. C., and Ray, M. J. (1997) Truncation of the amino terminus of human apolipoprotein A-I substantially alters only the lipid-free conformation, *Biochemistry 36*, 288−300.
42. Tanaka, M., Saito, H., Dhanasekaran, P., Wehrli, S., Handa, T., Lund-Katz, S., and Phillips, M. C. (2005) Effects of the core lipid on the energetics of binding of ApoA-I to model lipoprotein particles of different sizes, *Biochemistry 44*, 10689−10695.
43. Arnulphi, C., Jin, L., Tricerri, M. A., and Jonas, A. (2004) Enthalpy-driven apolipoprotein A-I and lipid bilayer interaction indicating protein penetration upon lipid binding, *Biochemistry 43*, 12258−12264.
44. Frank, P. G., and Marcel, Y. L. (2000) Apolipoprotein A-I: Structure−function relationships, *J. Lipid Res. 41*, 853−872.
45. Fang, Y., Gursky, O., and Atkinson, D. (2003) Structural studies of N- and C-terminally truncated human apolipoprotein A-I, *Biochemistry 42*, 6881−6890.
46. Tricerri, M. A., Agree, A. K. B., Sanchez, S. A., and Jonas, A. (2000) Characterization of apolipoprotein A-I structure using a cysteine-specific fluorescence probe, *Biochemistry 39*, 14682−14691.
47. Gross, E., Peng, D. Q., Hazen, S. L., and Smith, J. D. (2006) A novel folding intermediate state for apolipoprotein A-I: Role of the amino and carboxy termini, *Biophys. J. 90*, 1362−1370.
48. Krishna, M. M., and Englander, S. W. (2005) The N-terminal to C-terminal motif in protein folding and function, *Proc. Natl. Acad. Sci. U.S.A. 102*, 1053−1058.
49. Agree, A. K. B., Tricerri, M. A., McGuire, K. A., Tian, S.-M., and Jonas, A. (2002) Folding and stability of the C-terminal half of apolipoprotein A-I examined with a Cys-specific fluorescence probe, *Biochim. Biphys. Acta 1594*, 286−296.
50. Lazar, K. L., Miller-Auer, H., Getz, G. S., Orgel, J. P., and Meredith, S. C. (2005) Helix−turn−helix peptides that form α-helical fibrils: Turn sequences drive fibril structure, *Biochemistry 44*, 12681−12689.
51. Sorci-Thomas, M. G., and Thomas, M. J. (2002) The effects of altered apolipoprotein A-I structure on plasma HDL concentration, *Trends Cardiovasc. Med. 12*, 121−128.
52. Genschel, J., Haas, R., Propsting, M. J., and Schmidt, H. H. (1998) Apolipoprotein A-I induced amyloidosis, *FEBS Lett. 430*, 145−149.
53. Hatters, D. M., and Howlett, G. J. (2002) The structural basis for amyloid formation by plasma apolipoproteins: A review, *Eur. Biophys. J. 31*, 2−8.
54. Hatters D. M., MacPhee, C. E., Lawrence, L. J., Sawyer, W. H., and Howlett, G. J. (2000) Human apolipoprotein C-II forms twisted amyloid ribbons and closed loops, *Biochemistry 39*, 8276−8283.
55. Oda, M. N., Forte, T. M., Ryan, R. O., and Voss, J. C. (2003) The C-terminal domain of apolipoprotein A-I contains a lipid-sensitive conformational trigger, *Nat. Struct. Biol. 10*, 455−460.
56. Gorshkova, I. N., Liu, T., Zannis, V. I., and Atkinson, D. (2002) Lipid-free structure and stability of apolipoprotein A-I: Probing the central region by mutation, *Biochemistry 41*, 10529−10539.
57. Gorshkova I. N., Liu, T., Kan, H. Y., Chroni, A., Zannis, V. I., and Atkinson, D. (2006) Structure and stability of apolipoprotein A-I in solution and in discoidal high-density lipoprotein probed by double charge ablation and deletion mutation, *Biochemistry 45*, 1242−1254.
58. Pearson, K., Saito, H., Woods, S. C., Lund-Katz, S., Tso, P., Phillips, M. C., and Davidson W. S. (2004) Structure of human apolipoprotein A-IV: A distinct domain architecture among exchangeable apolipoproteins with potential functional implications, *Biochemistry 43*, 10719−10729.
59. Pearson, K., Tubb, M. R., Tanaka, M., Zhang, X. Q., Tso, P., Weinberg, R. B., and Davidson, W. S. (2005) Specific sequences in the N and C termini of apolipoprotein A-IV modulate its conformation and lipid association, *J. Biol. Chem. 280*, 38576−38582.

BI060726T